Simulation of the proton component below the geomagnetic cutoff detected by the AMS experiment

L. Derome, M. Buenerd

Simulation of the proton component below the geomagnetic cutoff detected by the AMS experiment

L. Derome and M. Buénerd[a]

[a]Institut des Sciences Nucléaires
53 av. des Martyrs, 38026 Grenoble cedex, France

The high flux proton component observed by AMS below the geomagnetic cutoff can be well accounted for by assuming these particles to be secondaries originating from the interaction of cosmic ray protons with the atmosphere. The simulation results are presented.

1. Introduction

The existence of a high flux proton component below the earth geomagnetic cutoff (GC), was reported recently by the AMS collaboration [1], and successfully accounted for in ref [2], referred to as paper 1 below. Such a subGC component has to be a secondary product of the primary cosmic ray (CR) flux on earth [3]. Since the experiment was running on a 370 km orbit, the quasi identity between subGC upward and downward flux indicate that this flux is at least partly trapped in the earth field.

2. Simulation

The inclusive spectrum of cosmic ray at the altitude of AMS has been calculated by means of a computer simulation program built to this purpose. This communication reports on some numerical and physical improvements of paper 1 calculations. Cosmic ray particles were generated isotropically on a sphere at 500 km altitude, with their natural abundance and momentum distributions [4] corrected for the solar modulation effect [5]. Each particle is then backtraced trough the geomagnetic field. This inverted technique allows to select particles coming from the outer space. This saves a significant amount of computing time. The propagation includes a detailed treatment of the effect of the geomagnetic field and of the multipolar features of the field [6]. Forbidden trajectories intersecting the earth surface are properly treated.

At this stage, the proton cosmic ray incident flux is considered as the only source of secondary protons (see ref [2]). Particles are allowed to interact with atmospheric nuclei (mainly ^{14}N and ^{16}O, see ref [7] for the model of atmosphere), and to produce secondary nucleons.

The invariant proton and neutron production cross sections in pA and nA collisions was described by means of the parametization proposed in [8] (QE, Quasi-Free component):

$$\frac{E}{\sigma}\frac{d^3\sigma_{QF}}{d^3p} = CA^{b(p_t)}x'(1-x')^{\alpha p_t^2}(p_t^2+\mu^2)^{-4.5} \text{ where } b(p_t) = \begin{cases} b_0 p_t & \text{for} \quad p_t \leq \Gamma \\ b_0\Gamma & \text{for} \quad p_t > \Gamma \end{cases} \tag{1}$$

The values of paramters b_0, Γ, μ^2, C and α are given in table 1. The kinematic variables used in this relation are $x' = E_*/E_{*max}$ and p_t, where E_* and E_{*max} are the total energy and its maximum possible value in the nucleon-nucleon center of mass respectively, p_t being the transferred transverse momentum.

Since this parametrisation is not expected to account for the very low energy and backward proton emission (DI, Deep-Inelastic component), the latter was included using the following parametrization [9] :

$$E\frac{d^3\sigma_{DI}}{d^3p} = C_b\left(\frac{A}{12}\right)^{1.3} \exp\left[-\frac{(T-T_0)(1-\beta\cos\theta)}{T_1}\right] \tag{2}$$

where the parameters C_b, T_0, T_1 and β are given in table 1. The kinematic variables used in this parametrization are the kinetic energy T and the emission angle θ, of the secondary particle.

Table 1
Values of the parameters used in equations 1 and 2

μ^2	b_0	Γ	C	α	C_b	T_1	β	T_0
1.3	.13	5.0	2.27	1.14	371	57	0.59	22.7

Figure 1 shows the two components, QE (dotted line), and DI (dashed line), for 125 MeV protons from $p+C$ at 7.5 GeV/c, compared to the data at the same energy ($*$-symbol) [9]. It is seen that the sum of the two components (solid line) compares pretty well to the data, providing a sound cross-section input to the calculations. The arrow shows the location of the kinematic limit in the reaction $pp \rightarrow pX$ with 125 MeV proton in the final state. The discrepancy around the kinematic limit may be tentatively assigned to the fermi motion in the target nucleus. It will be included later in the calculation.

Each secondary particle is then propagated and allowed to collide as in paper 1. A reaction cascade can thus develop through the atmosphere. The reaction products are counted whenever they cross upward or downward, the virtual sphere at the AMS altitude. Particles are counted each time they cross the sphere of detection altitude. This may bring large statistical weights for trapped particles.

3. Results and conclusion

Figure 2 shows the experimental kinetic energy distributions for downward and upward protons, measured for all latitude bins, compared to the results of two simulations runs : one using only the QE component for secondaries (dotted line) and the second using the two components QE+DI (solid line). No free parameter was used for normalization to the data. The results are entirely determined by the physics input to the calculation.

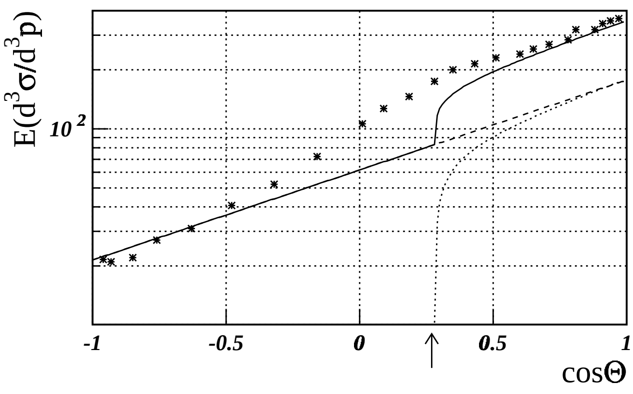

Figure 1. Angular dependence of the invariant cross section for 125 MeV proton production in *pC* collision: QE component from eq. 1 (dotted line) and DI component from eq. 2 (solid line). The sum of the two components (solid line) is compared to the data from [9].

The figure clearly shows that a good agreement is obtained on the average, between the simulated results and the data, both for upward and downward protons. It is also seen that the DI component provides a major contribution to the subGC component at the lowest proton energies as it could be expected, and that the DI contribution to the cross section cannot be ignored or neglected. These successful results also demonstrate the correctness of the physical basis of the simulation. The deficit of the simulated yield observed for the subGC components in the equatorial region can be tentatively assigned to the deficit of the calculated cross section around and below the kinematic limit. More work is in progress on the subject.

REFERENCES

1. J. Alcaraz et al., Phys. Lett. B472 (2000) 215
2. L. Derome et al., Phys. Lett. B489 (2000) 1
3. C. Störmer, The Polar Aurora, Clarendon Press (Cambridge), 1955; See also M.S. Vallarta, Handbuch der Physik, Springer Verlag, Vol 61/1, p 88, 1961.
4. J.A. Simpson, Ann. Rev. Nucl. and Part. Sci. 33 (1983) 323; B. Wiebel-Sooth, P.L. Biermann, and H. Meyer, A&A, 330 (1997) 389
5. J.S. Perko, Astro. Astrophys. 184(1984)119; see M.S. Potgieter, Proc. ICRC Calgary, 1993, p213, for a recent review of the subject.
6. N.A. Tsyganenko, J. Geophys. Res. 100 (1995) 5599; N.A. Tsyganenko ans D.P. Stern, J. Geophys. Res. 101 (1996) 27187
7. A.E. Hedin, J. Geophys. Res. 96 (1991) 1159
8. A. N. Kalinovsky, N. V. Mokhov and Y. P. Nikitin, “Passage Of High-Energy Particles Through Matter” NEW YORK, USA: AIP 1989.
9. Y.D. Bayukov et al., Sov. J. of Nuc. Phys. 42 (1985) 116

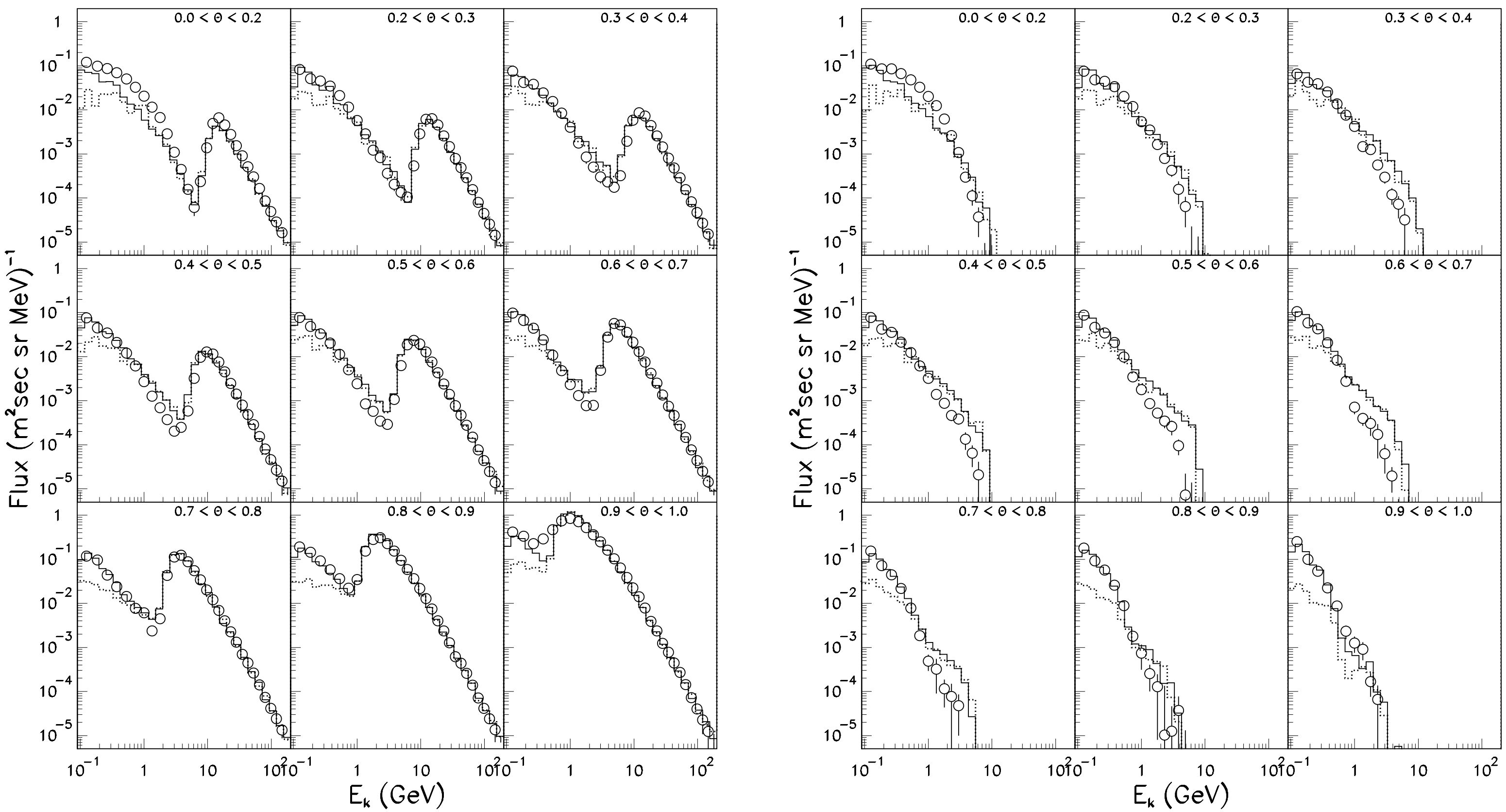

Figure 2: Experimental kinetic energy distributions from [1] for a sample of bins in latitudes (open circles), compared to the results of two simulations (dotted line (QE) and full line (QE+DI)) described in the text, for downward (left) and upward (right) protons.